Effect of ferroelectric-poling-induced strain on the phase separation and magnetotransport properties of $La_{0.7}Ca_{0.15}Sr_{0.15}MnO_3$ thin films grown on ferroelectric single-crystal substrates

R. K. Zheng,[1,2,*] H.-U. Habermeier,[1] H. L. W. Chan,[2] C. L. Choy,[2] and H. S. Luo[3]
[1]*Max Planck Institute for Solid State Research, Heisenbergstrasse 1, D-70569 Stuttgart, Germany*
[2]*Department of Applied Physics and Materials Research Center, The Hong Kong Polytechnic University, Hong Kong, China*
[3]*State Key Laboratory of High Performance Ceramics and Superfine Microstructure, Shanghai Institute of Ceramics, Chinese Academy of Sciences, Shanghai 201800, China*
(Received 9 May 2009; revised manuscript received 9 July 2009; published 25 September 2009)

We report the effects of the ferroelectric-poling-induced strain on the phase separation, magnetic, and magnetotransport properties of $La_{0.7}Ca_{0.15}Sr_{0.15}MnO_3$ (LCSMO) thin films grown on ferroelectric $0.67Pb(Mg_{1/3}Nb_{2/3})O_3$-$0.33PbTiO_3$ (PMN-PT) single-crystal substrates. *In situ* x-ray diffraction measurements show that the ferroelectric poling induces a reduction in the in-plane tensile strain in the LCSMO film, which gives rise to a decrease in the resistance and an increase in the ferromagnetism and Curie temperature T_C. The induced reduction in the tensile strain leads to opposite effect on the magnetoresistance below and above T_C. Based on a phenomenogical model that well reproduces the essential features of the field- and temperature-dependence of the resistance of the LCSMO film when the PMN-PT substrate is in unpoled and poled state, respectively, we found that the volume fraction of the ferromagnetic metallic phase is significantly enhanced due to the reduction in the in-plane tensile strain in the film. We discuss these strain effects within the framework of the electron-lattice coupling and phase separation scenario that are relevant to the strain induced by the ferroelectric poling.

DOI: 10.1103/PhysRevB.80.104433 PACS number(s): 75.47.Lx, 75.47.Gk, 77.22.Ej, 77.80.−e

I. INTRODUCTION

Colossal magnetoresistance (CMR) manganites $La_{1-x}A_xMnO_3$ (A=Ca,Sr,Ba) have attracted considerable attention due to their interesting physical properties and possible device applications.[1] Although the properties of manganites have been extensively studied in the last decade, some fundamental aspects of their physical behaviors are still not fully understood. In particular, the underlying mechanism for the phase separation, i.e., coexistence of ferromagnetic metallic (FMM) and charge-ordered antiferromagnetic insulating (AFI) or paramagnetic insulating (PMI) phases within the same sample, and its influence on the magnetoresistance (MR) are still under investigation. Recent studies indicate that many variables can strongly influence the energy balance between the coexisting phases and therefore affects the magnetic and transport properties of manganite thin films. Tebano *et al.*[2] studied the effects of the in-plane compressive strain on the phase separation in $La_{0.7}Sr_{0.3}MnO_3$ thin films grown on $LaAlO_3$ substrates and found that, with decreasing film thickness from 39 to 12 nm, the substrate-induced in-plane compressive strain induces an $3z^2-r^2$ orbital ordered *C*-type AFI phase in the FMM matrix, which strongly influences the magnetic and transport properties of the films. In contrast, Gillaspie *et al.*[3] found that the substrate-induced in-plane compressive strain suppresses the charge-ordered insulating phase and favors the FMM phase in phase-separated $La_{0.325}Pr_{0.3}Ca_{0.375}MnO_3$ films. Bibes *et al.*[4] reported that, irrespective of whether the substrate-induced strain is compressive or tensile, with decreasing film thickness from 108 to 2.4 nm, the resistivity and the low-temperature MR increases while the metal-to-insulator transition temperature T_P decreases systematically in $La_{0.67}Ca_{0.33}MnO_3$ films grown on different types of substrates. They concluded that the phase separation arising from the differences in growth mechanisms and the disorders in Mn-O bond lengths and Mn-O-Mn bond angles at the interface induced by the different atomic terminations of the uppermost atomic layers of the substrate is responsible for the transport and magnetic properties of the films. Biswas and co-workers[5,6] reported that the nonuniform distribution of the strain due to the three-dimensional growth mode of the films induces a charge-ordered insulating phase in the FMM matrix in $La_{0.67}Ca_{0.33}MnO_3$ films grown on $LaAlO_3$ substrates, which consequently suppresses the ferromagnetism of the films. Similar findings have been reported for $La_{0.67}Ca_{0.33}MnO_3$ films grown on $SrLaAlO_4$ substrates with in-plane compressive strain by Peña *et al.*[7] Moreover, Ogale *et al.*[8] found that oxygen deficiency can result in a significant change in the microscopic constitution of the electronic and magnetic phases in $(La_{0.6}Pr_{0.4})_{0.7}Ca_{0.3}MnO_3$ films. These results demonstrate that the phase separation phenomena in manganite thin films is quite complex and is discussed controversially. In order to obtain more insight into the intrinsic effects of the substrate-induced strain on phase separation and MR, it is necessary to investigate the properties of manganite thin films using the same thin-film sample so that certain extrinsic effects, such as those induced by different types of substrates, growth modes, atomic terminations of substrate surface, and oxygen nonstoichiometry, can be kept constant.

In this paper, we studied the effects of the substrate-induced strain on the phase separation and MR of epitaxial $La_{0.7}Ca_{0.15}Sr_{0.15}MnO_3$ (LCSMO) thin films grown on ferroelectric $0.67Pb(Mg_{1/3}Nb_{2/3})O_3$-$0.33PbTiO_3$ (PMN-PT) single-crystals substrates. Here, the ferroelectric poling *in situ* induces an in-plane compressive strain in the PMN-PT substrate. The induced strain is simultaneously transferred to

 ©2009 The American Physical Society

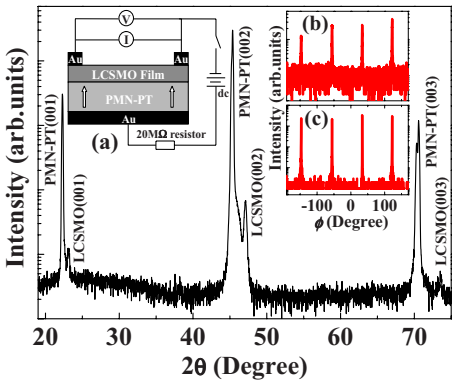

FIG. 1. (Color online) X-ray diffraction pattern of the LCSMO/PMN-PT structure. Inset (a) shows a schematic diagram of the LCSMO/PMN-PT structure and the electrical measurement circuit. The arrow in the inset (a) represents the poling direction. Inset (b) and (c) show the XRD ϕ scans on the LCSMO(101) and PMN-PT(101) reflections, respectively.

the film, thus the in-plane tensile strain in the film is reduced, which results in a significant decrease in the resistance and an increase in the ferromagnetism and Curie temperature (T_C) of the film. Furthermore, it was found that the induced reduction in the in-plane tensile strain leads to opposite effect on MR below and above T_C, namely, MR is reduced for $T<T_C$ while MR is enhanced for $T>T_C$. These induced strain effects were closely related to the Jahn-Teller (JT) electron-lattice coupling that is relevant to the strain induced by the ferroelectric poling.

II. EXPERIMENTAL DETAILS

The PMN-PT single crystals were grown by a modified Bridgman technique[9] at the Shanghai Institute of Ceramics. The crystals were cut into small plates (10 mm$\times$2.5 mm $\times$0.5 mm) with the plate normal in the $\langle 001 \rangle$ crystal direction and polished to a surface roughness less than 1 nm. LCSMO films were deposited on the (001)-oriented and polished PMN-PT substrates using dc magnetron sputtering. The deposition was carried out in an argon-oxygen flow with 60% Ar and 40% O_2 at a pressure of 5 Pa and a substrate temperature of 700 °C. After deposition, the films were cooled to room temperature and postannealed in 1 atm of flowing O_2 at 700 °C for 30 min using a rapid thermal processor furnace. Although the lattice constants ($a\sim b\sim c \sim 4.02$ Å) (Ref. 10) of the PMN-PT substrate are larger than those of the LCSMO bulk material, i.e., $a\sim b\sim c \sim 3.888$ Å,[11] it is still possible to epitaxially grow perovskite manganite thin films, e.g., $La_{1-x}A_xMnO_3$ (A=Ca,Sr), on (1 $-x$)PMN-xPT single-crystal substrates,[12–15] as revealed by x-ray diffraction (XRD). The thickness of these films is estimated to be $\sim$65 nm. XRD patterns of the PMN-PT substrate and LCSMO film were recorded using a four-circle Bruker D8 Discover x-ray diffractometer equipped with Cu Kα_1 radiation.

The inset (a) of Fig. 1 is a schematic diagram of the LCSMO/PMN-PT structure and the electrical measurement circuit. A physical property measurement system (PPMS, Quantum Design) was used to measure the resistance of the film between the two top-top gold electrodes in the temperature range 25–325 K and in a magnetic field (up to 8 Tesla) applied parallel to the film plane. Measurements of the leakage current in the PMN-PT substrate using a Keithley 6517A electrometer indicate that the resistance of the PMN-PT substrate is $\sim 3\times 10^9$ Ω at room temperature. Compared to the huge resistance of the PMN-PT substrate, the resistance ($\sim 3.6\times 10^3$ Ω at room temperature) of the LCSMO film can be reasonably neglected, namely, the conducting LCSMO film in fact serves as the top electrode in the LCSMO/PMN-PT structure.[13] The poling of the PMN-PT substrate was achieved by applying a dc poling field E to the LCSMO/PMN-PT structure through the top LCSMO film (held at low potential) and the bottom gold electrode (held at high potential) using a Model PS325 high-voltage power supply (Stanford Research Systems, Inc.) and the same electric measurement circuit shown in the inset (a) of Fig. 1. The magnetic properties of the LCSMO film were measured using a superconducting quantum interference device (SQUID, Quantum Design) magnetometer with the magnetic field applied parallel to the film plane.

III. RESULTS AND DISCUSSION

Figure 1 shows the XRD pattern of the LCSMO/PMN-PT structure when the PMN-PT substrate is in the unpoled state (denoted by P_r^0). The XRD pattern indicates that the film is highly (001)-oriented and has no secondary phases. The out-of-plane or c-axis lattice constant of the film calculated from the LCSMO(002) reflection is $\sim$3.856 Å. This value is smaller than the c-axis lattice constant ($c\sim 3.888$ Å)[11] of the LCSMO bulk material, indicating that the film is subjected to an out-of-plane compressive ($\varepsilon_{zz}=-0.82\%$) and in-plane tensile strain, consistent with the fact that the lattice constants of the LCSMO bulk material are smaller than those ($a\sim b\sim c \sim 4.02$ Å) of the PMN-PT substrate. XRD ϕ scans on the LCSMO(101) and PMN-PT(101) reflections were also performed. A fourfold symmetry is seen for both the LCSMO film and the PMN-PT substrate, as shown in the inset (b) and (c) of Fig. 1, respectively, which indicates a cube-on-cube epitaxial growth of the LCSMO film on the PMN-PT substrate.

The effects of the strain induced by the ferroelectric poling on the transport properties of the LCSMO film were characterized by measuring the resistance of the film between the two top-top gold electrodes as a function of the electric field E applied to the LCSMO/PMN-PT structure through the top and bottom electrodes [see inset (a) of Fig. 1] at a fixed temperature of 294 K. It is noted that the PMN-PT substrate was initially in P_r^0 state and the electric field E was increased from 0 to 8 kV/cm in steps of 0.2 kV/cm. In Fig. 2, we show the relative change in the resistance, $\Delta R/R$, of the film as a function of E. Here, $\Delta R/R$ is defined as $\Delta R/R=[R(E)-R(0)]/R(0)$ where $R(E)$ and $R(0)$ are the resistance of the film under an electric field E and zero electric field, respectively. One sees that the resistance is almost field independent for $E\leq 2.2$ kV/cm, but decreases drastically with increasing E from 2.2 to 3 kV/cm and decreases gently with

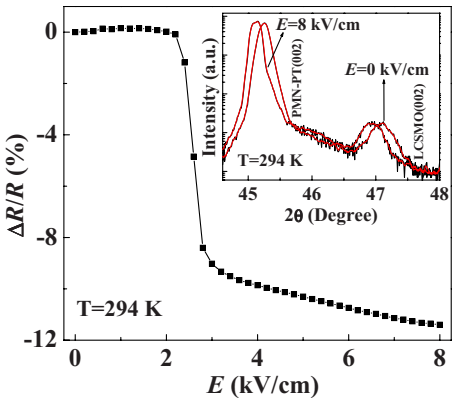

FIG. 2. (Color online) Relative change in the resistance of the LCSMO film between the two top-top gold electrodes at 294 K as a function of the electric fields applied to the LCSMO/PMN-PT structure through the top and bottom electrodes. Inset shows the XRD patterns for the LCSMO/PMN-PT structure under zero electric field and an electric field of 8 kV/cm. The PMN-PT substrate is initially in P_r^0 state.

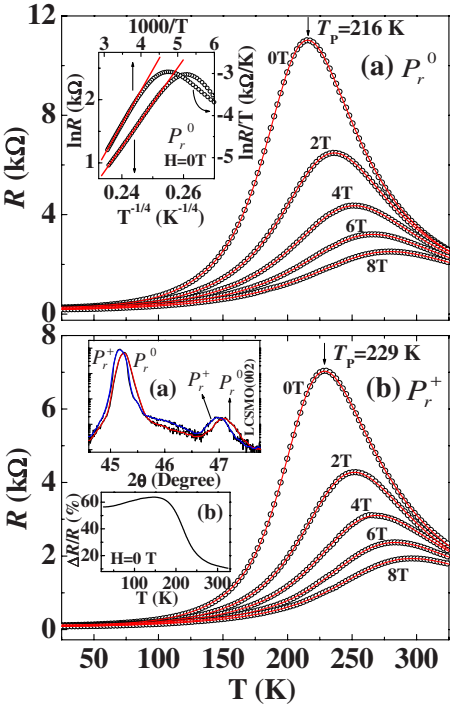

FIG. 3. (Color online) (a) Temperature-dependence of the resistance for the LCSMO film at $H=0$, 2, 4, 6, and 8 T when the PMN-PT substrate is in P_r^0 state. The solid lines are the fitted results using Eq. (1). The inset in (a) shows $\ln R$ vs $T^{-1/4}$ and $\ln R/T$ vs $1000/T$ curves at $H=0$ T and when the PMN-PT substrate is in P_r^0 state. (b) Temperature-dependence of the resistance for the LCSMO film at $H=0$, 2, 4, 6, and 8 T when the PMN-PT substrate is in P_r^+ state. The solid lines are the fitted results using Eq. (1). Inset (a) shows the XRD patterns for the LCSMO/PMN-PT structure when the PMN-PT substrate is in P_r^0 and P_r^+ state, respectively. Inset (b) shows the relative change in the resistance, $\Delta R/R$, of the film. Here, $\Delta R/R=[R(P_r^0)-R(P_r^+)]/R\ (P_r^0)]$. Note that the poling field was turned off after the PMN-PT substrate had been poled to P_r^+ state.

further increase in E. Such a large electric-field-induced decrease in the resistance is similar to that observed in $La_{0.875}Ba_{0.125}MnO_3$/PMN-PT structure[16] and is probably due to a reduction in the in-plane tensile strain in the film induced by the alignment of the ferroelectric domains toward the field direction in the PMN-PT substrate. This is confirmed by *in situ* XRD measurements on the LCSMO/PMN-PT structure using the same electric configuration as that shown in the inset (a) of Fig. 1. The XRD measurements were made during the application of an electric field E ($0 \le E \le 8$ kV/cm) to the LCSMO/PMN-PT structure through the top and bottom electrodes. Note that the PMN-PT substrate was initially in P_r^0 state. With increasing electric field from 0 to 8 kV/cm, we found that both the c-axis lattice constants of the PMN-PT substrate and the LCSMO film increase, as reflected by the shift of the 2θ angles of the PMN-PT(002) and LCSMO(002) reflections to lower values (see the selected XRD patterns shown in the inset of Fig. 2). For $E=8$ kV/cm, the c-axis lattice constant of the film is measured to be ~3.869 Å, which is closer to but still smaller than that of the LCSMO bulk material. This indicates that the film is still under out-of-plane compressive ($\varepsilon_{zz}=-0.49\%$) and in-plane tensile strain, although the in-plane tensile strain has been significantly reduced as a result of the ferroelectric poling. Using the expression $\varepsilon_{zz}=-2\nu/(1-\nu)\varepsilon_{xx}$, where ε_{zz}, ε_{xx}, and ν are the out-of-plane strain, in-plane strain, and Poisson's ratio, respectively, and assuming approximate volume preserving distortion, i.e., $\nu=0.5$, for the LCSMO film, the induced change in the in-plane tensile strain $\delta\varepsilon_{xx}$ [defined as $\delta\varepsilon_{xx}=\varepsilon_{xx}(E)-\varepsilon_{xx}(0)$] is ~−0.165% for $E=8$ kV/cm. Therefore, the reduction in the in-plane tensile strain in the film induced by the ferroelectric poling should be responsible for the transport behavior of the film shown in Fig. 2.

Figures 3(a) and 3(b) show the temperature-dependence of the resistance for the LCSMO film in different magnetic fields H when the PMN-PT substrate is in P_r^0 and P_r^+ state (i.e., the polarization direction in the PMN-PT substrate points to the film), respectively. When the PMN-PT substrate is in P_r^0 state and $H=0$ T, the resistance of the film increases with decreasing temperature from 325 K and undergoes an insulator-to-metal transition at $T_P \sim 216$ K, exhibiting the typical transport behaviors of CMR materials. After the measurements of the resistance of the LCSMO film as a function of temperature in different magnetic fields when the PMN-PT substrate is in P_r^0 state, we poled the PMN-PT substrate by applying an electric field of 10 kV/cm to the PMN-PT substrate through the top and bottom electrodes at room temperature and turned off the electric field after the PMN-PT substrate has been poled for 10 min. It is interesting to find that, after the PMN-PT substrate has been poled to P_r^+ state, T_P of the film increases significantly and the resistance is reduced in the whole temperature range. The relative change in the resistance, $\Delta R/R$, [here, $\Delta R/R=[R(P_r^0)-R(P_r^+)]/R(P_r^0)]$ of the film between P_r^0 and P_r^+ state at $H=0$ T is shown in the inset (b) of Fig. 3(b).

According to the low-temperature XRD results obtained from the PMN-PT polycrystalline sample and the phase diagram of $(1-x)$PMN-xPT proposed by Noheda *et al.*,[10] there is no structural phase transition for $T \le 300$ K. Nevertheless,

with increasing temperature from 20 to 300 K, the lattice constants of the PMN-PT substrate changes smoothly by ~0.01 Å.[10] This value is the same as that (~0.01 Å)[17,18] observed in the extensively used $SrTiO_3$ single-crystal substrates. Moreover, all the transport and magnetic data reported in this paper were obtained from the same piece of LCSMO/PMN-PT structure. So, the change in the lattice constants with temperature when the PMN-PT substrate was in P_r^0 state is the same as that when the PMN-PT substrate was in P_r^+ state. Therefore, the effects of the changes in the lattice constants of the PMN-PT substrate with temperature on the transport and magnetic properties of the LCSMO film could be neglected.

As pointed out by Ahn *et al.*,[19] the poling of the ferroelectrics in manganite/ferroelectrics heterostructures would give rise to a depletion or accumulation of the charge carriers in the manganite film and hence influence the transport and magnetic properties of the film. The polarization-field-induced change in the charge carrier density Δn can be estimated using $\Delta n = \Delta P/ed$,[20] where ΔP is the remnant polarization of the PMN-PT substrate, e is the unit charge, and d is the thickness of the LCSMO film. Using $\Delta P \sim 32\ \mu C/cm^2$ and $d \sim 65$ nm, one obtains $\Delta n \sim 3.1 \times 10^{19}/cm^3$. Assuming a moderate charge carrier density of $n = 5 \times 10^{21}/cm^3$ for the LCSMO film, we obtain $\Delta n/n \sim 0.6\%$. Assuming that the relative change in the resistance is proportional to the relative change in the charge carrier density, i.e., $\Delta R/R \approx \Delta n/n$,[21,22] it is estimated that the polarization-field-induced change in the resistance is ~0.6%. Since the polarization direction points to the LCSMO film, the holes in the film would be depleted by the polarization field. Thus, if one only considers the ferroelectric field effect, the resistance of the film should increase by ~0.6%. Nevertheless, in real practice, the sign of the change in the resistance is opposite to that expected from the ferroelectric field effect, and moreover, the observed $\Delta R/R$ [see inset (b) of Fig. 3(b)] is much larger than 0.6%. Furthermore, provided that the ferroelectric field effect plays a dominant role in influencing the transport properties of the film, the resistance electric field (R-E) hysteresis loop should show a squarelike shape, as previously observed in $La_{1-x}Ba_xMnO_3 (x = 0.1, 0.15)/Pb(Zr_{0.2}Ti_{0.8})TiO_3$ (Ref. 22) and $La_{0.8}Ca_{0.2}MnO_3/Pb(Zr_{0.2}Ti_{0.8})TiO_3$ (Ref. 23) ferroelectric field effect transistor structures. To obtain further insight into the ferroelectric field effect in the LCSMO/PMN-PT structure, we measured the R-E hysteresis loop of the LCSMO/PMN-PT structure and show the results in Fig. 4. The R-E hysteresis loop shows a butterflylike shape, which is the typical behavior of the resistance due to the strain induced by the rotation of the polarization direction in the PMN-PT substrate. Similar butterflylike R-E hysteresis loop has been observed in $La_{0.7}Sr_{0.3}MnO_3/0.72Pb(Mg_{1/3}Nb_{2/3})O_3$-$0.28PbTiO_3$ structure.[12] Thus, we believe that the ferroelectric field effect in the LCSMO/PMN-PT structure is minor and negligible.[13]

Since the ferroelectric Curie temperature of the PMN-PT substrate is ~155 °C (much higher than room temperature), the polarization direction in the PMN-PT substrate will still point toward the poling direction even if the poling field was turned off. As a consequence, there is a remnant strain in the

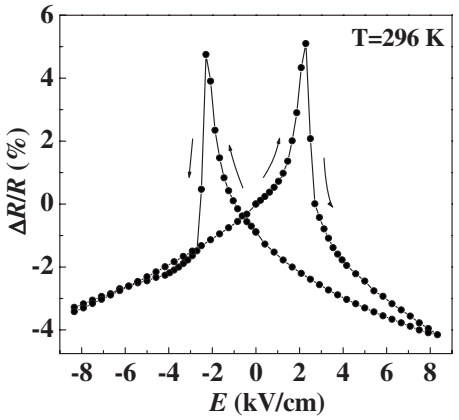

FIG. 4. Relative change in the resistance of the LCSMO film between the two top-top gold electrodes at 296 K as a function of bipolar electric field applied to the PMN-PT substrate through the top and bottom electrodes. The PMN-PT substrate was initially in P_r^+ state and the electric field was changed in the sequence of 0 kV/cm → −8.3 kV/cm → +8.3 kV/cm → 0 kV/cm.

PMN-PT substrate, as reflected by the shift of the PMN-PT(002) reflection toward lower 2θ value [inset (a) of Fig. 3(b)]. The remnant strain has been transferred to the film, causing a contraction of the in-plane lattice constants and an expansion of the out-of-plane lattice constant of the LCSMO film, which is reflected by the shift of the LCSMO(002) reflection toward lower 2θ value [inset (a) of Fig. 3(b)]. The XRD results show that the c-axis lattice constant of the film increases from 3.856 Å for P_r^0 state to 3.864 Å for P_r^+ state, corresponding to a decrease in the in-plane tensile strain from 0.41% to 0.31%, (i.e., $\delta\varepsilon_{xx} = -0.1\%$). All these results indicate that the ferroelectric-poling-induced remnant strain in the PMN-PT substrate should be responsible for the reduction in the in-plane tensile strain, the decrease in the resistance and the increase in the Curie temperature of the LCSMO film, in agreement with the theoretical calculations by Millis *et al.*[24] and Perroni *et al.*[25] who showed that a small reduction in the biaxial strain could induce a large decrease in the resistance and an enhancement in the transition temperature in the CMR region for manganite films.

Figure 5 shows the temperature-dependence of MR at $H = 2$, 4, and 8 T when the PMN-PT substrate is in P_r^0 and P_r^+ states, respectively. Here, MR is defined as $MR = [R(0) - R(H)]/R(0)$ where $R(0)$ and $R(H)$ are the resistance of the film in zero magnetic field and a magnetic field H, respectively. It is interesting to note that the MR versus T curves for P_r^0 and P_r^+ states have a crossover near T_C at any H value, indicating that a reduction in the in-plane tensile strain leads to opposite effect on MR above and below T_C, namely, MR is reduced in the ferromagnetic state while MR is enhanced in the paramagnetic state. To get a clearer understanding of the effects of the induced strain on MR, we measured MR of the film at various fixed temperatures covering the range from the ferromagnetic state to paramagnetic state. Figure 6 shows MR versus H curves at several temperatures when the PMN-PT substrate is in P_r^0 and P_r^+ state, respectively. The results clearly indicate that, in comparison with the MR when the PMN-PT substrate is in P_r^0 state, the MR value

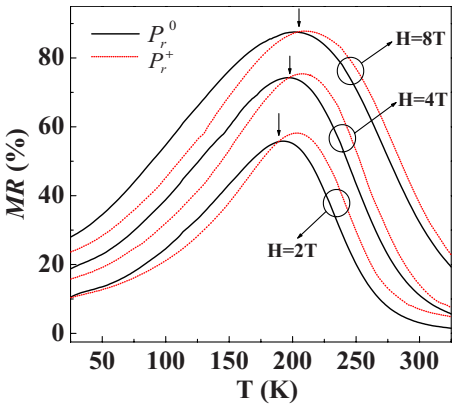

FIG. 5. (Color online) Temperature-dependence of MR for the LCSMO film at $H=2$, 4, and 8 T when the PMN-PT substrate is in P_r^0 and P_r^+ state, respectively.

when the PMN-PT substrate is in P_r^+ state is reduced in the ferromagnetic state (e.g., 9, 91, 146, and 200 K) but enhanced in the paramagnetic state (e.g., 216, 245, 274, 306, and 325 K), consistent with the behaviors of the MR versus T curves shown in Fig. 5.

A wide variety of experimental results and theoretical calculations have convincingly demonstrated that manganites, especially those displaying insulator-to-metal transition and CMR effect, intrinsically phase separates into PMI and FMM phases.[26–29] For $T \gg T_C$, the materials are in the PMI state. Upon cooling to a characteristic temperature T_{onset} ($T_{onset} > T_C$), the ferromagnetically coupled Mn^{3+}-O-Mn^{4+} pairs start to segregate into larger ferromagnetic regions within a paramagnetic matrix and grow in size with decreasing temperature. At T_C, the competition between the PMI phase and the FMM phase reaches a balance. Upon further cooling from T_C, the FMM phase further grows at the expense of the PMI phase, and thus dominates over the PMI phase in ferromagnetic state. Assuming that these phase separation behaviors exist in the LCSMO film and following the phenomenogical model that describes the phase separation below and above T_C proposed by Yuan *et al.*[30] and Li *et al.*,[31] the total resistance of the LCSMO film can be considered as a serial combination of the resistance of the coexisting phases and can be expressed as

$$R = f_{FM} R_{FM} + (1 - f_{FM}) R_{PM}, \tag{1}$$

where f_{FM} and $(1-f_{FM})$ are the volume fractions of the FMM phase and the PMI phase, and R_{FM} and R_{PM} are the resistance of the FMM phase and the PMI phase, respectively. The temperature-dependence of f_{FM} obeys a two energy-level Boltzmann distribution and can be expressed as[30,31]

$$f_{FM} = \frac{1}{1 + \exp(\Delta U / k_B T)}, \tag{2}$$

where ΔU is the energy difference between the FMM phase and the PMI phase and can be written as

$$\Delta U = - U_0(H, \varepsilon_{xx})[1 - T/T_P^{\mathrm{mod}}(H, \varepsilon_{xx})], \tag{3}$$

where T_P^{mod} is the insulator-to-metal transition temperature used in the phenomenogical model and is close to T_P of the film, and U_0 is the energy difference between the FMM phase and the PMI phase at $T=0$ K. Combining Eq. (2) with Eq. (3), we obtain

$$f_{FM} = \frac{1}{1 + \exp[U_0 / k_B (1/T_P^{\mathrm{mod}} - 1/T)]}. \tag{4}$$

It is clear that, at the low temperature ($T \ll T_P^{\mathrm{mod}}$), $f_{FM} \sim 1$ while at high temperature ($T \gg T_P^{\mathrm{mod}}$), $f_{FM} \sim 0$.

In the high-temperature region ($T > T_P$), it is found that, whether the PMN-PT substrate is in P_r^0 or P_r^+ state, the resistance data are well fitted to the equation derived from the variable-range-hopping (VRH) model

$$R_{PM}(T) = C \exp[(T_0/T)^{1/4}], \tag{5}$$

where T_0 is a characteristic temperature and C is a constant. The inset in Fig. 3(a) shows the ln R vs $T^{-1/4}$ curve when the PMN-PT substrate is in P_r^0 state and $H=0$ T. We have also fitted these resistance data to the expression derived from the small polaron model: $R(T) = R_0 T \exp(E_a / k_B T)$ [see the inset of Fig. 3(a)]. We found that the resistance data can be linearly fitted in the temperature range from 245 to 325 K and 261 to 325 K using the VRH and the small polaron model, respectively, indicating that the VRH model gives a better description of the resistance data for $T > T_P$ than the small polaron model. In the low-temperature FMM state, previous studies have shown that the resistance can be ascribed to the contributions from (a) residual resistance R_0, (b) single-magnon's scattering term AT^2, and (c) electron-phonon interaction term BT^5, so the resistance can be expressed as[32]

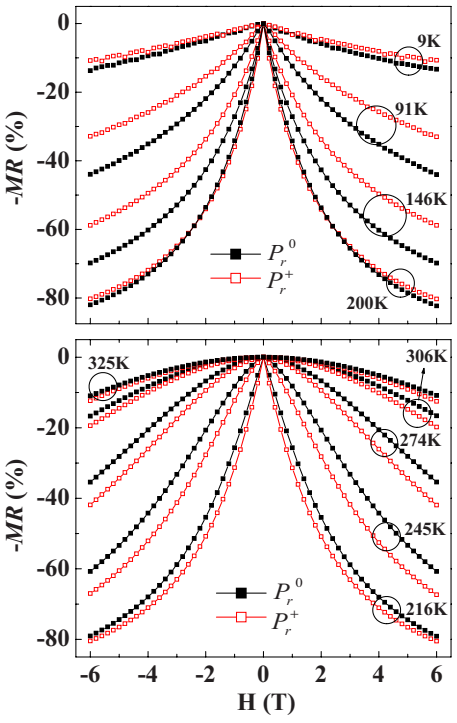

FIG. 6. (Color online) MR versus H curves at several temperatures for the LCSMO film when the PMN-PT substrate is in P_r^0 and P_r^+ state, respectively.

TABLE I. Summary of the fitted values of the parameters R_0, A, B, C, U_0/k_B, T_P^{mod}, and T_0 for the LCSMO film at H=0, 2, 4, 6, and 8 T when the PMN-PT substrate is in P_r^0 state.

H (T)	R_0 (kΩ)	A (kΩ K^{-2})	B (kΩ K^{-5})	C (kΩ)	U_0/k_B (K)	T_P^{mod} (K)	T_0 (K)
0	0.26	2×10^{-5}	2.19×10^{-11}	2.27×10^{-7}	3078.5	215.8	2.09×10^{7}
2	0.22	2×10^{-5}	9.06×10^{-12}	7.66×10^{-7}	3046.4	239.7	1.39×10^{7}
4	0.19	2×10^{-5}	4.50×10^{-12}	3.88×10^{-6}	2980.8	257.8	7.7×10^{6}
6	0.18	2×10^{-5}	2.53×10^{-12}	9.99×10^{-7}	2926.6	273.8	4.86×10^{6}
8	0.17	1×10^{-5}	1.53×10^{-12}	6.43×10^{-7}	2917.5	290.1	4.57×10^{6}

$$R_{FM}(T) = R_0 + AT^2 + BT^5. \quad (6)$$

Putting Eqs. (4)–(6) into Eq. (1), we fitted the temperature- and field-dependence of the resistance for the LCSMO film in the temperature region from 25 to 325 K when the PMN-PT substrate is in P_r^0 and P_r^+ state, respectively. The values of the fitting parameters obtained are shown in Tables I and II, respectively. The solid lines in Figs. 3(a) and 3(b) are the fitted results, which agree well with the experimental data.

Putting the values of the parameters U_0/k_B and T_P^{mod} shown in Tables I and II into Eqs. (4), we obtain the temperature- and field-dependent volume fraction of the FMM phase when the PMN-PT substrate is in P_r^0 and P_r^+ state, respectively (see Fig. 7). The essential features of the temperature-dependence of f_{FM} in different magnetic fields are similar to those of the f_{FM} values of $La_{0.67}Ca_{0.33}MnO_3$ extracted from the resistivity data using the effective-medium approximation method by Jaime *et al.*[32] One sees that, associated with the ferroelectric poling, the volume fraction of the FMM phase in different magnetic fields is significantly enhanced. As discussed above, when the PMN-PT substrate is in P_r^0 state, the film is subjected to an out-of-plane compressive and in-plane tensile strain, which indicates that the MnO_6 octahedra are compressed along c axis and elongated in the film plane.[33] This strain-induced biaxial distortion of MnO_6 octahedra tends to localize the charge carriers due to the JT electron-lattice coupling, as pointed out by Millis *et al.*[24] When the in-plane tensile strain is reduced due to the ferroelectric poling, the biaxial distortion of the MnO_6 octahedra will decrease, so the JT electron-lattice coupling strength is weakened and the delocalization and hopping of charge carriers are favored.[24,34,35] This, in turn, would enhance the ferromagnetism and T_C of the film since the double-exchange-induced ferromagnetism demands the active hopping of charge carriers. As shown in Fig. 8 and the inset (a) and (b) of Fig. 8, both the magnetization and T_C of the film are enhanced significantly associated with the reduction in the in-plane tensile strain induced by the ferroelectric poling, which is consistent with the above picture.

Now, if the phase separation scenario and the electron-lattice coupling that are relevant to the strain induced by the ferroelectric poling are taken into account, the opposite effect of the induced strain on MR below and above T_C can be understood as follows. At T_C, the FMM phase strongly competes with the PMI phase and the volume fraction of these two phases reaches a balance. The critical ratio of f_{FM} to $(1-f_{FM})$ [i.e., $\lambda_C=f_{FM}/(1-f_{FM})$] is optimal at T_C where MR shows the maximal value. It is clear that, if the value of $f_{FM}/(1-f_{FM})$ is larger or smaller than λ_C, MR would decrease, namely, the closer the value of $f_{FM}/(1-f_{FM})$ to λ_C, the larger the MR. Whether the LCSMO film is in the PMI state or the FMM state, a reduction in the electron-lattice coupling would enhance f_{FM}. In the high-temperature PMI state, the value of $f_{FM}/(1-f_{FM})$ should be less than λ_C because the PMI phase dominates over the FMM phase with respect to that at T_C. So, the increase in f_{FM} would cause the value of $f_{FM}/(1-f_{FM})$ to be closer to λ_C, thereby enhancing MR. Nevertheless, in the low-temperature FMM state ($T<T_C$), the increase in f_{FM} would cause the value of $f_{FM}/(1-f_{FM})$ ever larger than λ_C, thereby reducing MR.

IV. CONCLUSIONS

In summary, using ferroelectric PMN-PT single crystals as substrates, we have studied the intrinsic effects of

TABLE II. Summary of the fitted values of the parameters R_0, A, B, C, U_0/k_B, T_P^{mod}, and T_0 for the LCSMO film at H=0, 2, 4, 6, and 8 T when the PMN-PT substrate is in P_r^+ state.

H (T)	R_0 (kΩ)	A (kΩ K^{-2})	B (kΩ K^{-5})	C (kΩ)	U_0/k_B (K)	T_P^{mod} (K)	T_0 (K)
0	0.12	5.98×10^{-5}	8.42×10^{-12}	6.08×10^{-7}	3338.4	223.3	1.65×10^{7}
2	0.10	7.26×10^{-5}	3.98×10^{-12}	1.07×10^{-7}	3316.5	249.6	1.32×10^{7}
4	0.09	8.08×10^{-5}	2.10×10^{-12}	5.59×10^{-6}	3337.7	267.0	7.83×10^{6}
6	0.08	7.16×10^{-5}	1.13×10^{-12}	2.0×10^{-5}	3200.8	278.5	5.40×10^{6}
8	0.08	6.57×10^{-5}	7.33×10^{-13}	1.0×10^{-5}	3129.5	292.5	5.31×10^{6}

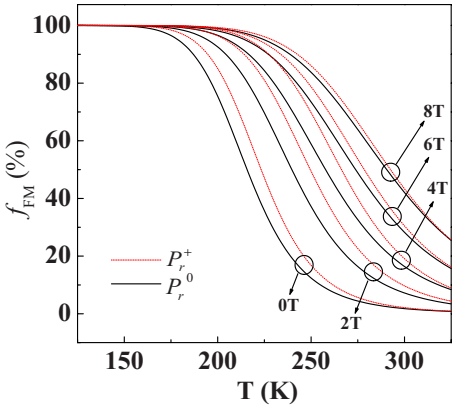

FIG. 7. (Color online) Temperature-dependence of the volume fraction of the FMM phase at $H=0$, 2, 4, 6, and 8 T when the PMN-PT substrate is in P_r^0 and P_r^+ state, respectively.

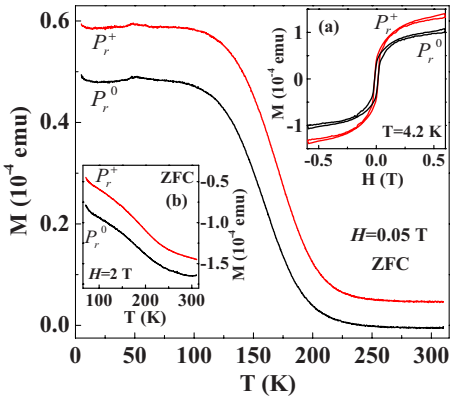

FIG. 8. (Color online) Temperature-dependence of the zero-field-cooled magnetization (M) for the LCSMO/PMN-PT structure at $H=0.05$ T when the PMN-PT substrate is in P_r^0 and P_r^+ state, respectively. Inset (a) shows the magnetization loop of the LCSMO/PMN-PT structure at 4.2 K when the PMN-PT substrate is in P_r^0 and P_r^+ state, respectively. Inset (b) shows zero-field-cooled M vs T curves of the LCSMO/PMN-PT structure at $H=2$ T when the PMN-PT substrate is in P_r^0 and P_r^+ state, respectively.

substrate-induced strain on the phase separation, magnetic, and magnetotransport properties of LCSMO thin films by *in situ* inducing strain in the film via the ferroelectric poling of the PMN-PT substrate. The ferroelectric poling leads to a reduction in the in-plane tensile strain in the film, giving rise to a weakening of the electron-lattice coupling and thus a decrease in the resistance and an increase in the ferromagnetism and T_C of the film. The induced reduction in the in-plane tensile strain leads to opposite effect on MR below and above T_C, namely, MR is reduced for $T<T_C$ while MR is enhanced for $T>T_C$. These strain effects on magnetic and magnetotransport properties are closely related to the phase separation which is found to be suppressed in the ferromagnetic state but enhanced in the paramagnetic state as a result of the ferroelectric-poling-induced strain.

ACKNOWLEDGMENTS

This work was supported by Max Planck Institute for Solid State Research, the Hong Kong Research Grants Council (Grant No. CERG PolyU 5122/07E), and the Center for Smart Materials of the Hong Kong Polytechnic University. One of us (R.K.Z.) is highly indebted to the Alexander von Humboldt Foundation.

*zrk@ustc.edu

[1] M. B. Salamon and M. Jamie, Rev. Mod. Phys. **73**, 583 (2001).
[2] A. Tebano, C. Aruta, P. G. Medaglia, F. Tozzi, G. Balestrino, A. A. Sidorenko, G. Allodi, R. De Renzi, G. Ghiringhelli, C. Dallera, L. Braicovich, and N. B. Brookes, Phys. Rev. B **74**, 245116 (2006).
[3] D. Gillaspie, J. X. Ma, H. Y. Zhai, T. Z. Ward, H. M. Christen, E. W. Plummer, and J. Shen, J. Appl. Phys. **99**, 08S901 (2006).
[4] M. Bibes, S. Valencia, L. Balcells, B. Martínez, J. Fontcuberta, M. Wojcik, S. Nadolski, and E. Jedryka, Phys. Rev. B **66**, 134416 (2002).
[5] A. Biswas, M. Rajeswari, R. C. Srivastava, Y. H. Li, T. Venkatesan, R. L. Greene, and A. J. Millis, Phys. Rev. B **61**, 9665 (2000).
[6] A. Biswas, M. Rajeswari, R. C. Srivastava, T. Venkatesan, R. L. Greene, Q. Lu, A. L. de Lozanne, and A. J. Millis, Phys. Rev. B **63**, 184424 (2001).
[7] V. Peña, Z. Sefrioui, D. Arias, C. León, J. Santamaria, M. Varela, S. J. Pennycook, M. Garcia-Hernandez, and J. L. Martinez, J. Phys. Chem. Solids **67**, 472 (2006).
[8] A. S. Ogale, S. R. Shinde, V. N. Kulkarni, J. Higgins, R. J. Choudhary, D. C. Kundaliya, T. Polleto, S. B. Ogale, R. L. Greene, and T. Venkatesan, Phys. Rev. B **69**, 235101 (2004).
[9] Z. W. Yin, H. S. Luo, P. C. Wang, and G. S. Xu, Ferroelectrics **229**, 207 (1999).
[10] B. Noheda, D. E. Cox, G. Shirane, J. Gao, and Z.-G. Ye, Phys. Rev. B **66**, 054104 (2002).
[11] The lattice constants $a\sim b\sim c\sim 3.888$ Å was obtained by Rietveld refinement of the powder x-ray diffraction pattern of the LCSMO ceramic target for sputtering.
[12] C. Thiele, K. Dörr, S. Fähler, L. Schultz, D. C. Meyer, A. A. Levin, and P. Paufler, Appl. Phys. Lett. **87**, 262502 (2005).
[13] C. Thiele, K. Dörr, O. Bilani, J. Rödel, and L. Schultz, Phys. Rev. B **75**, 054408 (2007).
[14] R. K. Zheng, J. Wang, X. Y. Zhou, Y. Wang, H. L. W. Chan, C. L. Choy, and H. S. Luo, J. Appl. Phys. **99**, 123714 (2006).
[15] R. K. Zheng, Y. Wang, H. L. W. Chan, C. L. Choy, and H. S. Luo, Appl. Phys. Lett. **90**, 152904 (2007).
[16] R. K. Zheng, Y. Wang, H. L. W. Chan, C. L. Choy, and H. S. Luo, Appl. Phys. Lett. **92**, 082908 (2008).
[17] F. W. Lytle, J. Appl. Phys. **35**, 2212 (1964).
[18] For $SrTiO_3$ substrate, using $\alpha=1/L\times\Delta L/\Delta T$ where α is the thermal expansion coefficient of the $SrTiO_3$ substrate, L ($\sim$3.905 Å) is the lattice constant of the $SrTiO_3$ substrate, $\alpha\approx 9.4\times 10^{-6}$/K,[17] and ΔT ($\sim$280 K) is the change in temperature, it is estimated that the lattice constant of $SrTiO_3$ substrate

changes by ~0.01 Å with increasing temperature from 20 to 300 K.

[19] C. H. Ahn, A. Bhattacharya, M. D. Ventra, J. N. Eckstein, C. D. Frisbie, M. E. Gershenson, A. M. Goldman, I. H. Inoue, J. Mannhart, A. J. Millis, A. F. Morpurgo, D. Natelson, and J.-M. Triscone, Rev. Mod. Phys. **78**, 1185 (2006).

[20] K. S. Takahashi, D. Matthey, D. Jaccard, J.-M. Triscone, K. Shibuya, T. Ohnishi, and M. Lippmaa, Appl. Phys. Lett. **84**, 1722 (2004).

[21] C. H. Ahn, R. H. Hammond, T. H. Geballe, M. R. Beasley, J.-M. Triscone, M. Decroux, Ø. Fischer, L. Antognazza, and K. Char, Appl. Phys. Lett. **70**, 206 (1997).

[22] T. Kanki, Y.-G. Park, H. Tanaka, and T. Kawai, Appl. Phys. Lett. **83**, 4860 (2003).

[23] T. Zhao, S. B. Ogale, S. R. Shinde, R. Ramesh, R. Droopad, J. Yu, K. Eisenbeiser, and J. Misewich, Appl. Phys. Lett. **84**, 750 (2004).

[24] A. J. Millis, T. Darling, and A. Migliori, J. Appl. Phys. **83**, 1588 (1998).

[25] C. A. Perroni, V. Cataudella, G. De Filippis, G. Iadonisi, V. Marigliano Ramaglia, and F. Ventriglia, Phys. Rev. B **68**, 224424 (2003).

[26] J. Burgy, A. Moreo, and E. Dagotto, Phys. Rev. Lett. **92**, 097202 (2004).

[27] J. M. D. Teresa, M. R. Ibarra, P. A. Algarabel, C. Ritter, C. Marquina, J. Blasco, J. García, A. D. Moral, and Z. Arnold, Nature (London) **386**, 256 (1997).

[28] M. Fäth, S. Freisem, A. A. Menovsky, Y. Tomioka, J. Aarts, and J. A. Mydosh, Science **285**, 1540 (1999).

[29] M. Uehara, S. Mori, C. H. Chen, and S.-W. Cheong, Nature (London) **399**, 560 (1999).

[30] S. L. Yuan, Z. Y. Li, W. Y. Zhao, G. Li, Y. Jiang, X. Y. Zeng, Y. P. Yang, G. Q. Zhang, F. Tu, C. Q. Tang, and S. Z. Jin, Phys. Rev. B **63**, 172415 (2001).

[31] G. Li, H.-D. Zhou, S. J. Feng, X. J. Fan, X. G. Li, and Z. D. Wang, J. Appl. Phys. **92**, 1406 (2002).

[32] M. Jaime, P. Lin, S. H. Chun, M. B. Salamon, P. Dorsey, and M. Rubinstein, Phys. Rev. B **60**, 1028 (1999).

[33] N. M. Souza-Neto, A. Y. Ramos, H. C. N. Tolentino, E. Favre-Nicolin, and L. Ranno, Phys. Rev. B **70**, 174451 (2004).

[34] X. J. Chen, S. Soltan, H. Zhang, and H.-U. Habermeier, Phys. Rev. B **65**, 174402 (2002).

[35] X. J. Chen, H.-U. Habermeier, H. Zhang, G. Gu, M. Varela, J. Santamaria, and C. C. Almasan, Phys. Rev. B **72**, 104403 (2005).